

# Spatialization of Instantaneous and daily average net radiation and Soil Heat Flux in the Territory of Itaparica, Northeast Brazil

Helio L. Lopes<sup>\*a</sup>, Bernardo B. Silva<sup>a</sup>, Antônio H. C. Teixeira<sup>b</sup>, Luciano J. O. Accioly<sup>c</sup>

<sup>a</sup>Universidade Federal de Pernambuco, Centro de Tecnologia e Geociências, Recife, Brazil;

<sup>b</sup>Embrapa Semiárido, Setor de Agrometeorologia, Petrolina, Brazil, <sup>c</sup>Embrapa Solos, Unidade de Execução e Pesquisa, Recife, Brazil

## ABSTRACT

This work has as aim to quantify the energy changes between atmosphere and surface by modeling both net radiation and soil heat flux related to land use and land cover. The methodology took into account modeling and mapping of physical and biophysical parameters using MODIS images and SEBAL algorithm in an area of native vegetation and irrigated crops. The results showed that there are variations in the values of the estimated parameters for different land cover types and mainly in caatinga cover. The dense caatinga presents mean values of soil heat flux ( $G_o$ ) of  $124.9 \text{ W m}^{-2}$  while sparse caatinga with incidence of erosion, present average value of  $132.6 \text{ W m}^{-2}$ . For irrigated plots cultivated with banana, coconut and papaya the mean  $G_o$  values were  $103.8$ ,  $98.6$  and  $113.9 \text{ W m}^{-2}$ , respectively. With regard to the instantaneous net radiation ( $R_n$ ), dense caatinga presented mean value of  $626.1 \text{ W m}^{-2}$ , while sparse caatinga a mean value of  $575.2 \text{ W m}^{-2}$ . Irrigated areas cultivated with banana, coconut and papaya presented  $R_n$  of  $658.1$ ,  $647.4$  and  $617.9 \text{ W m}^{-2}$ , respectively. Applying daily mean net radiation ( $R_{nDAve}$ ) it was found that dense caatinga had a mean value of  $417.1 \text{ W m}^{-2}$  while sparse caatinga had a mean value of  $379.9 \text{ W m}^{-2}$ . For the irrigated crops of banana, coconut and papaya the  $R_{nDAve}$  values were  $430.9$ ,  $431.3$  and  $411.6 \text{ W m}^{-2}$ , respectively. Sinusoidal model can be applied to determine the maximum and  $R_{nDAve}$  considering the diverse classes of LULC; however, there is a need to compare the results with field data for validation of this model.

**Key words:** biophysical parameters, land use and land cover (LULC), agrometeorology, sinusoidal model, MODIS.

## 1. INTRODUCTION

Net Radiation ( $R_n$ ) is related to radiative downward and upward fluxes of both short and longwave radiation that interact with Earth surface<sup>1</sup>.  $R_n$  is responsible for evaporation, photosynthesis and soil and air heating processes<sup>2</sup>. Continuous records of net radiation of Earth, in regional and global scale, were initially done as from 1978 by Nimbus satellite and nowadays by Earth Radiation Budget Experiment - ERBE and Earth's Radiant Energy System - CERES using multiple satellite data<sup>3</sup>. The spatial variation of  $R_n$  depends on land surface characteristics like: land use and land cover, surface albedo, soil moisture and temperature, among others<sup>4</sup>.

Input parameters of net radiation can be computed and spatialized by means of remote sensing techniques, in which sensors record solar radiation reflected by Earth surface considering spectral bands that are suitable for albedo and vegetation indices retrieving. Thermal information should be also recorded in order to compute surface temperature. Many of these recorded data has high spatial resolution, but in contradiction has low temporal resolution when compared with field observations<sup>2</sup>. Due to spatial feature and facility to obtain attributes from Earth surface, various investigators aimed to compute net radiation (and its input variables) by means of combining remote and field observations<sup>5, 6, 7, 1, 8</sup>.

For studies related to the retrieving of energy budget input parameters, measurements of net radiation are achieved frequently<sup>9, 10, 11, 12</sup>. Hence, Silva et al.<sup>7</sup> computed net radiation from semiarid of Brazil whereas Di Peace et al.<sup>13</sup> have analyzed the bias of topography in calculating net radiation. In this sense, Gomes et al.<sup>14</sup> evaluated alterations that replacement of natural vegetation by crops and forestry causes in the net radiations and energy budget.

\*heliovasf@hotmail.com; phone 0055 81 2126-8977; Fax: 0055 81 2126-8219; pós-civil/UFPE

Net radiation together with soil heat flux is a key parameter that drives evapotranspiration. To estimate  $R_n$ , surface temperature is commonly retrieved by using remote sensed data. In the actual algorithms, input parameters to determine  $R_n$  such as surface albedo, emissivity, air temperature, air emissivity and downwelling shortwave radiation need usually radiative transfer models, field observations or empirical supposition of certain parameters<sup>15</sup>.

Using agrometeorological station data, various parameters can be spatialized by applying interpolation techniques. Islam et al.<sup>16</sup> generated  $R_n$  map by means of interpolation of meteorological stations proceeding inverse distance weighted interpolation. The problem of this method is that a gradient is performed and do not represent the surface heterogeneity<sup>15</sup>. Thus, remote sensing provides variable information pixel by pixel in regional or global scale for various applications on environmental monitoring; taking advantages that field observation represents a small part of the study area. Thus, it becomes important to explore remote sensing data in order to overcome spatial problems commonly seen in conventional estimates of maximum and daily net radiation and soil heat flux. Thereby, this study aims spatializing instantaneous and daily average net radiation, and heat flux in different types of land use and land cover by MODIS imagery and SEBAL algorithm, along with a sinusoidal model.

## 2. MATERIAL AND METHODS

### 2.1 Study Area

The study area comprises both right and left banks of the Itaparica reservoir, covering parts of the states of Pernambuco (left bank) and Bahia (right bank). The combination of bands 1, 2 and 3 of MODIS is seen in Figure 1, which outlines the quadrant featuring the geographic location in the states of Pernambuco and Bahia. Geographically the area is inserted between the UTM/SAD-69 coordinates of 479500 and 613200 meters of longitude E and 9048500 and 8968500 meters of latitude N, pertaining to the 24S zone with central meridian -39°. The sampling points observed in the field to characterize land use and land cover are superimposed on MODIS image.

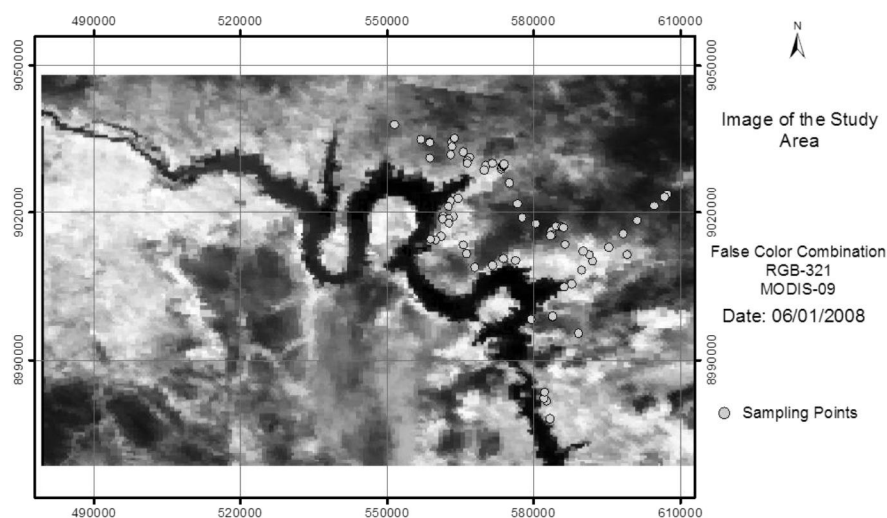


Figure 1. False color combination RGB-321 of MODIS (MOD09GA) image in gray scale for the study area.

### 2.2 Processing of orbital data

We use various land data products available from Terra-MODIS from 2008. The MODIS products were MOD09GA, MOD09GQ e MOD07A1. Data were converted into TIFF-sinusoidal projection and then reprojected to WGS84 geographical coordinates. Hereafter the image was cut in the shape of the study area and then imported to SPRING 5.2 software, in which each equation was written in LEGAL language. The layers imported into SPRING were: a) reflectance of bands 1 and 2 with 231.36 meters resolution, so that Normalized Difference Vegetation Index-NDVI, Soil Adjusted Vegetation Index-SAVI and Leaf Area Index-LAI could be determined; b) reflectances of bands from 1 to 7 with 463.31 meters resolution in order to spatialize surface albedo; c) surface temperature and emissivities of bands 31

and 32 with resolution of 926.63 meters, and also solar zenith angle data with the same last resolution. These resolutions were resampled to 250, 500 and 1000 meters.

### 2.3 Instantaneous net radiation modeling

Before proceeding the net radiation calculation (Equation 1) [17] various parameters were determined as emissivity ( $\epsilon_o$ ), downward longwave ( $L^\downarrow$ ) and shortwave radiation ( $K^\downarrow$ ), surface temperature ( $T_o$ ) and albedo ( $r_o$ ).

$$R_n = (1 - r_o)K^\downarrow + L^\downarrow - \epsilon_o \sigma T_o^4 - (1 - \epsilon_o)L^\downarrow \quad (1)$$

Net radiation as well as NDVI, surface albedo and temperature was used to compute soil heat flux-Go as shown in equation 2.

$$Go = \left[ \frac{T_o}{r_o} \times (0.0038r_o + 0.0074r_o^2)(1 - 0.98NDVI^4) \right] \times R_n \quad (2)$$

The maximum net radiation was determined by using equation 3 as shown by Bisht et al. [15].

$$R_{n\_max} = \frac{R_n}{\sin \times \left[ \left( \frac{t_{overpass} - t_{rise}}{t_{set} - t_{rise}} \right) \times \pi \right]} \quad (3)$$

where  $R_n$  is instantaneous net radiation,  $t_{overpass}$  is the satellite overpass hour,  $t_{rise}$  and  $t_{set}$  is the local time at which  $R_n$  value becomes positive and negative, respectively.

Daily average of net radiation was estimated applying equation 4 [15] as:

$$DANR = \frac{\int_{t_{rise}}^{t_{set}} R_n(t) dt}{\int_{t_{rise}}^{t_{set}} dt} = \frac{2R_{n\_max}}{\pi} = \frac{2INR}{\pi \sin \times \left[ \left( \frac{t_{overpass} - t_{rise}}{t_{set} - t_{rise}} \right) \times \pi \right]} \quad (4)$$

## 3. RESULTS

Soil heat flux throughout the study area is shown in Figure 2. There were values of Go for sparse vegetation and degraded soil of 126.6 e 132.6  $Wm^{-2}$ , respectively. For dense Caatinga, mean value of Go was 124.9  $Wm^{-2}$ , while for irrigated crops as coconut and banana, Go presents mean values of 103.8 e 98.6  $Wm^{-2}$ , respectively. For water bodies the mean value was 80  $Wm^{-2}$ .

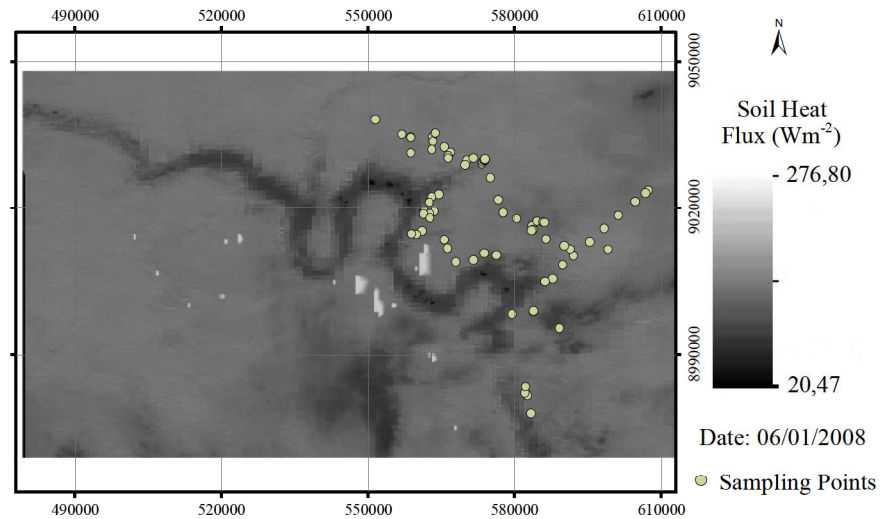


Figure 2. Soil heat flux throughout the study area at Itaparica reservoir.

Figure 3 shows descriptive statistics of each kind of land use and land cover regarded to soil heat flux.

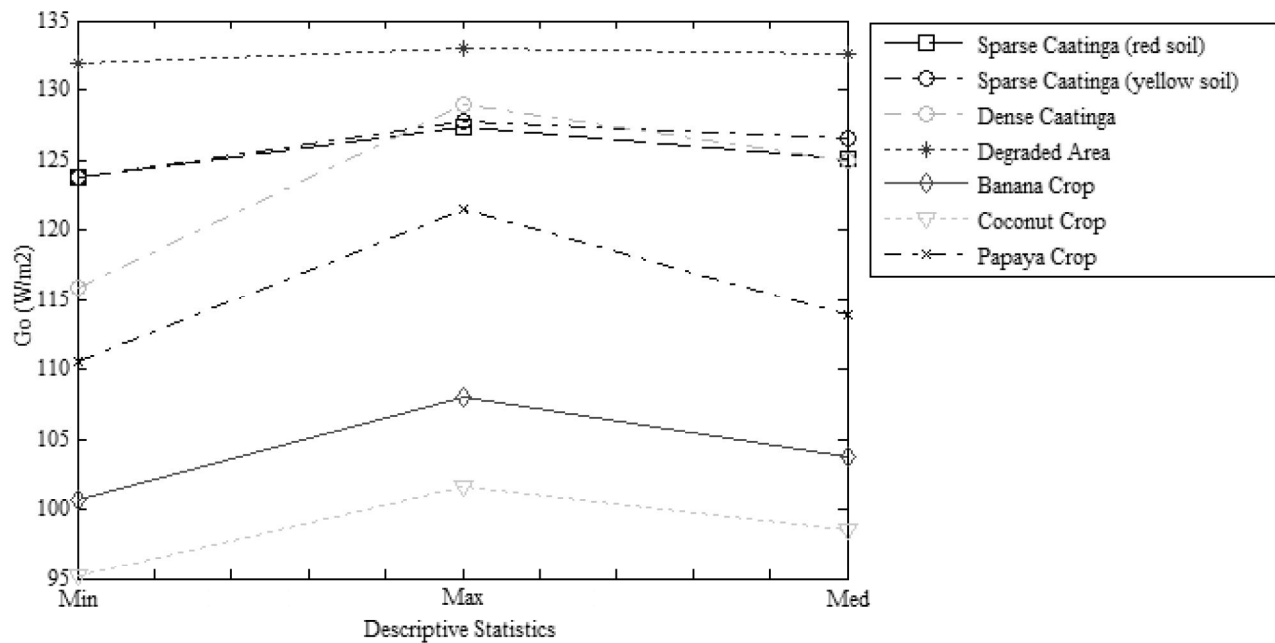


Figure 3. Graphic of descriptive statistics of  $G_o$ .

Areas with sparse caatinga that present different soil classes have low difference in the  $G_o$  values as shown in Figure 3. We can see that coconut areas have the lowest value of  $G_o$  (mean =  $98.6 \text{ Wm}^{-2}$ ) while degraded areas presented the highest values of  $G_o$  (mean =  $132.6 \text{ Wm}^{-2}$ ).

Figure 4 shows the spatial variation of instantaneous net radiation in the study area. It is noticed that areas with bare and degraded soil present low  $R_n$ , that correspond to darker areas on the map, while areas corresponding to water bodies such as Itaparica reservoir, are represented with shades whiter that corresponding to highest values. Areas in the Figure 4 with intermediate shades of gray correspond to high dense and dense caatinga whose mean values were  $626.1$  e  $728.0 \text{ W m}^{-2}$ , respectively.



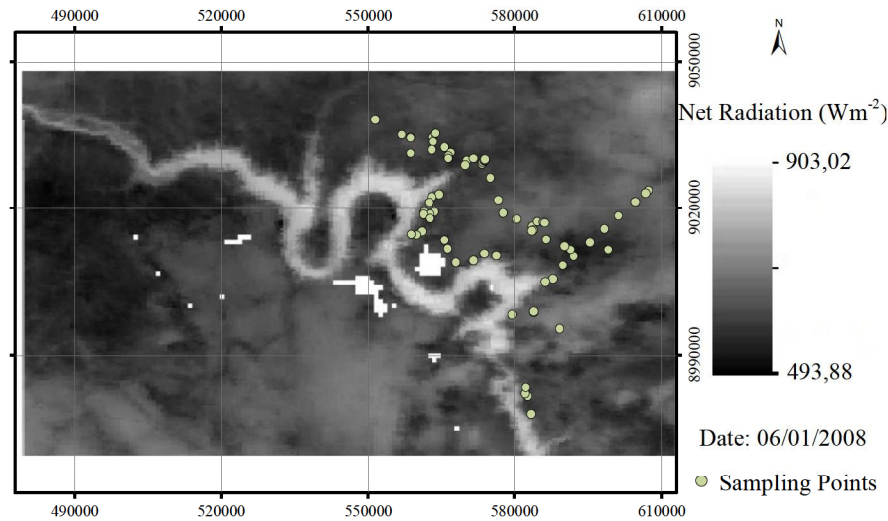


Figure 4. Map of instantaneous net radiation

According to what is seen in figure 4, it is noticed that there is variation in net radiation which may indicate that the time these variables become positive ( $t_{pos}$ ) and negative ( $t_{neg}$ ) vary with the type of land use and land cover, mainly in watershed which has a high surface heterogeneity. Thus, in this work is proposed an input of  $t_{pos}$  e  $t_{neg}$  take into account land use and land cover types. Thereby each pixel of land use and land cover has  $t_{pos}(x, y)$  e  $t_{neg}(x, y)$ . Consequently these variables are shown in Figure 5 which was proposed by Bisht et al.<sup>15</sup>, wherein the bold continuous curve represents the net radiation for a stated land use and land cover.

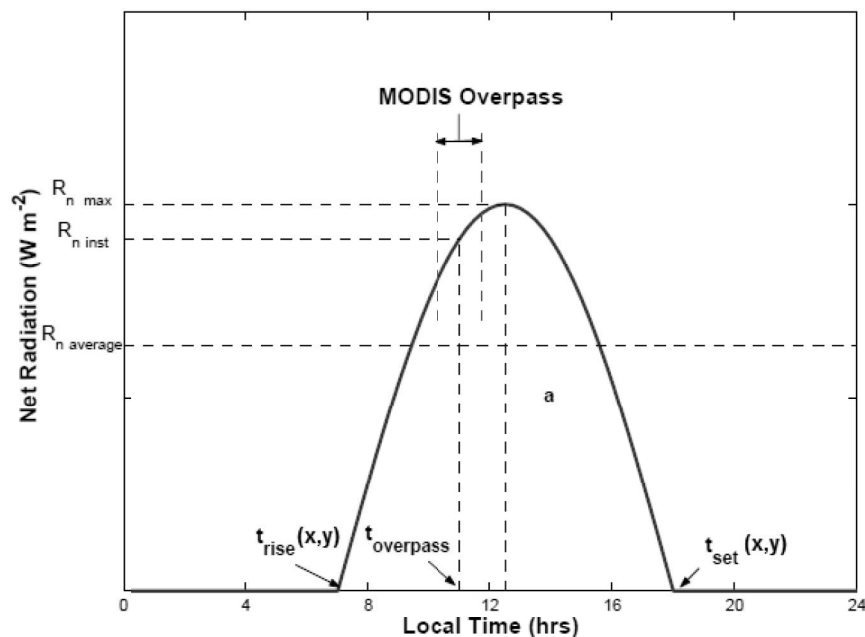


Figure 5. Sinusoidal model with MODIS overpass and  $t_{rise}$  and  $t_{set}$  considering each LULC pixel. After<sup>15</sup>.

The values represented by  $x$  and  $y$  denote the geographical position of pixel for each land use and land cover. To apply this procedure, it is necessary to generate the map of LULC, and from LULC layer set the values of each class related to  $t_{rise}$  and  $t_{set}$ , which to compute this task the  $t_{rise}$  and  $t_{set}$  values for each class need to be known, considering that thermal behavior of each class is variable. Research is needed aiming to determine both  $t_{rise}$  and  $t_{set}$  hours looking upon each

LULC, taking also into account soil classes since they have different thermal conductivity, specific heat and density in space and time<sup>18</sup>.

Figure 6 depicts the graphic of descriptive statistic regard to instantaneous net radiation as for LULC.

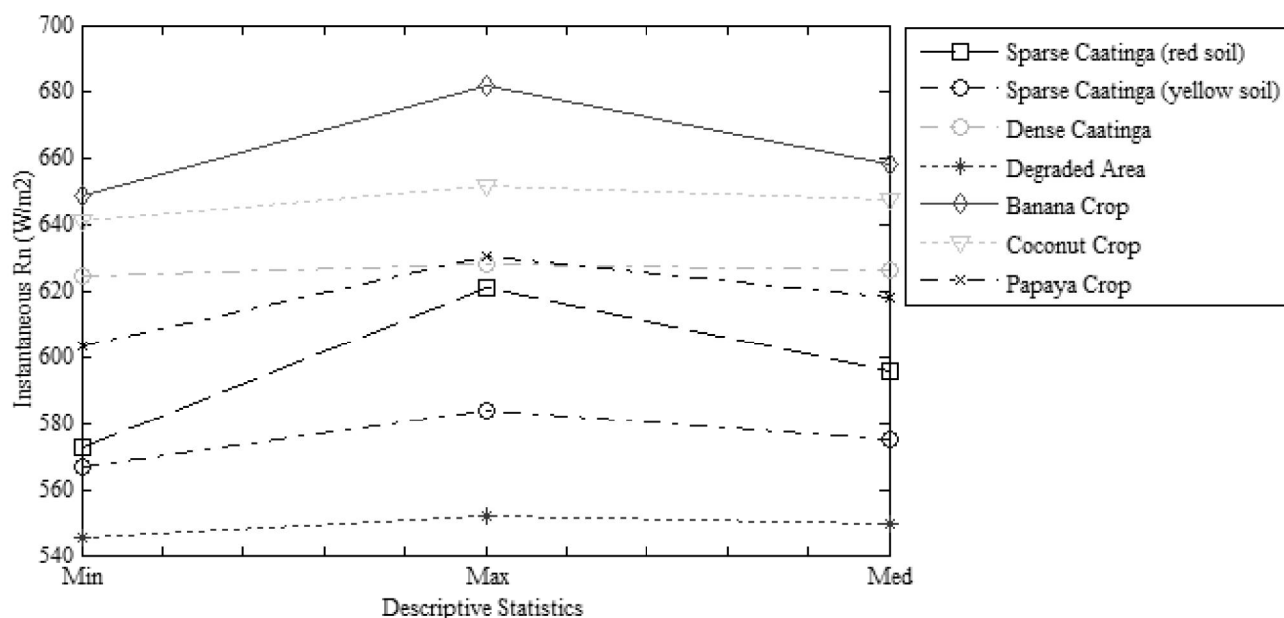


Figure 6. Graphic of instantaneous Rn regarding LULC.

In Figure 6 is observed that dense caatinga is fitted between irrigated field and degraded areas and sparse caatinga as to instantaneous net radiation values. Mean Rn values for dense caatinga, degraded areas and irrigated field (coconut) were 626.1, 549.7 e 647.4  $\text{Wm}^{-2}$ , respectively. Extreme values of Rn have been found to irrigated field (banana) with values of instantaneous  $Rn_{\min}$  equal to 648.6  $\text{Wm}^{-2}$  and  $Rn_{\max}$  de 681.4  $\text{Wm}^{-2}$ , and to degraded areas with instantaneous  $Rn_{\min}$  of 545.8  $\text{Wm}^{-2}$  and  $Rn_{\max}$  of 552.1  $\text{Wm}^{-2}$ . As regards sparse vegetation in which soil class was considered, it could be verified that there is a slight difference in that areas with red soils present higher descriptive statistical values of Rn as compared to areas with yellow soils. One reason for this difference may be caused by both NDVI and albedo which may vary as function of soil color since the shape of spectral reflectance curve is related to its color<sup>19</sup>, and therefore, to organic and inorganic constituents<sup>20</sup>.

Figura 7 shows the map of daily average net radiation  $Rn_{DAve}$  calculated from the sinusoidal model proposed by Bisht et al.<sup>15</sup>.  $Rn_{DAve}$  was spatialized in SPRING software using LEGAL language.

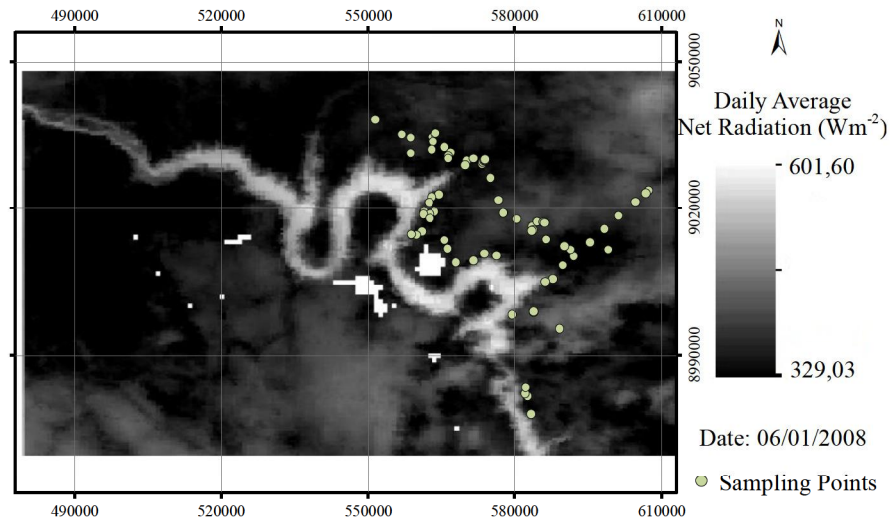


Figure 7. Daily average net radiation map for the study area.

The minimum and maximum values of  $R_{n\text{DAve}}$  were  $329.0 \text{ Wm}^{-2}$  and  $601.6 \text{ Wm}^{-2}$ , respectively. The high value is due to sinusoidal model super estimate the computed values in relation to observed values as seen in Bisht et al.<sup>15</sup>, may causing errors of 20% in some areas and  $R^2$  of 0.98 and 0.85 respectively for instantaneous  $R_n$  and daily average  $R_n$ .

Daily average net radiation is depicted in graphical form considering land use and land cover classes (Figure 8).

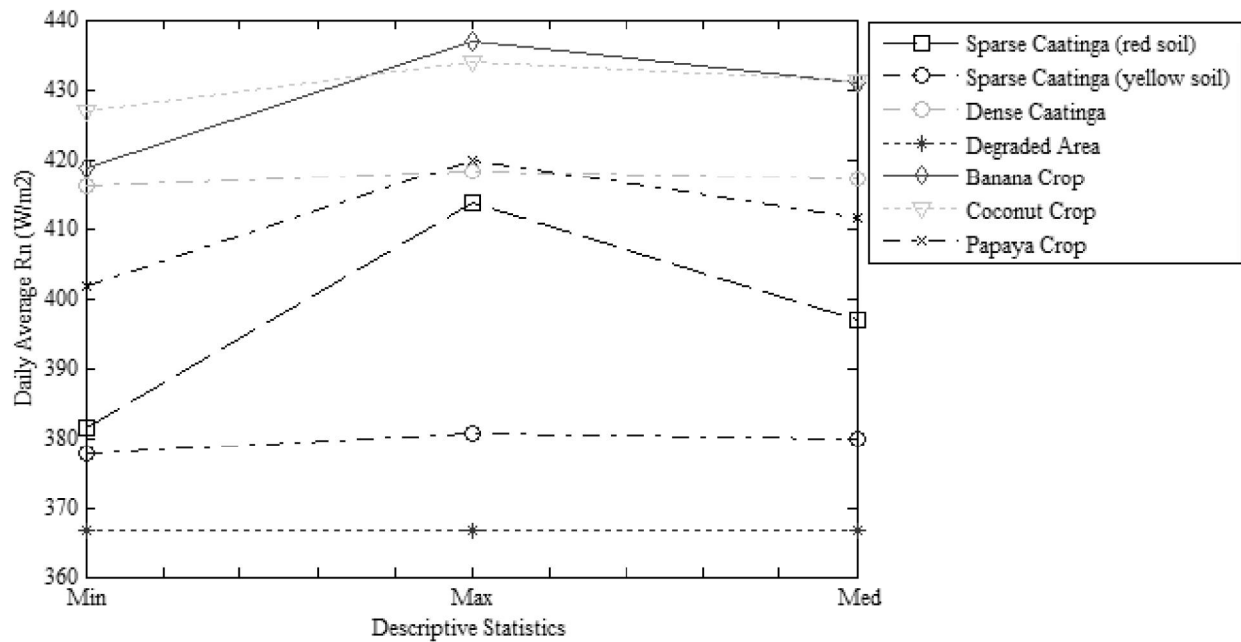


Figure 8. Descriptive statistic for daily average net radiation as for land use and land cover classes.

The behavior of  $R_{n\text{DAve}}$  is similar to the maximum  $R_n$  for all LULC classes. In studies conducted by Bisht et al.<sup>15</sup> the  $R_{n\text{DAve}}$  ranged from 205 to  $450 \text{ Wm}^{-2}$ , and was verified that the model tends to super estimate the values.

#### 4. CONCLUSIONS

In this work we applied equations to determine soil heat flux and net radiation (instantaneous, maximum, daily average). Net radiation was determined considering Terra/EOS satellite overpass as well as maximum and daily average net radiations were estimated using sinusoidal model and a comparison interclass of land use and land cover was done. It is observed that there is a need to a best knowledge of the model together with land use and land cover classes in order to validate with field observations taking into account each model variable as a function of LULC classes. Thereby, it becomes necessary to seek answers regarding the variables  $t_{rise}$  and  $t_{set}$  considering various LULC classes for each pixel. Studies are needed using these hypotheses in order to produce better optimization of the model. However it was found that it is possible to apply the sinusoidal model to determine the maximum and daily average net radiation taking into account the heterogeneity of LULC classes of caatinga ecosystem. Hence, there is a need to compare results from the model with field data in order to validate this model regarding to caatinga ecosystem and irrigated crops in a daily time behavior of each variable. No downscaling techniques were applied and spatial resolution of pixel should be considered when working on local scale in order to obtain better results.

#### 5. REFERENCES

- [1] Silva, B. B., Braga, A. C. and Braga, C. C., "Balanço de radiação no perímetro irrigado São Gonçalo – PB mediante imagens orbitais," *Rev. Caat* 24, 145-152 (2011).
- [2] Bisht, G. and Bras, R. L., "Estimation of net radiation from the MODIS data under all sky conditions: Southern Great Plains case study," *Remote Sensing of Environment*, 114, 1522–1534 (2010).
- [3] Ferreira, N. J., [Aplicações ambientais brasileiras dos satélites NOAA e Tiros-N], Oficina de Textos, São Paulo, (2004).
- [4] Aguiar, L. J. G., [Balanço de radiação em áreas de floresta e de pastagem em Rondônia], Universidade Federal de Viçosa, Viçosa, 70p (2007).
- [5] Jacobs, J. M., Myers, D. A., Anderson, M. C. and Diak, G. R., "GOES surface insolation to estimate wetlands evapotranspiration," *Journal of Hydrology*, 266, 53– 65 (2000).
- [6] Ma, Y., Su, Z., Li, Z., Koike, T. and Menenti, M., "Determination of regional net radiation and soil heat flux over a heterogeneous landscape of the Tibetan Plateau," *Hydrological Processes*, 16, 2963–2971 (2002).
- [7] Silva, B. B., Lopes, G. M. and Azevedo, P. V., "Determinação do albedo de áreas irrigadas com base em imagens Landsat 5 -TM," *Revista Brasileira de Agrometeorologia*, 13(2), 11-21 (2005).
- [8] Teixeira, A. H. de C., "Determining Regional Actual Evapotranspiration of Irrigated Crops and Natural Vegetation in the São Francisco River Basin (Brazil) Using Remote Sensing and Penman-Monteith Equation," *Remote Sensing*, 2(5), 1287-1319 (2010).
- [9] Azevedo, P. V., Silva, B. B. and Silva, V. P. R., "Water requirements of irrigated mango orchards in northeast Brazil," *Agricultural Water Management*, 58(3), 241-254 (2003).
- [10] Azevedo, P. V., Souza, C. B., Silva, B. B. and Silva, V. P. R., "Water requirements of pineapple crop grown in a tropical environment," *Agricultural Water Management*, 88(1-3), 201-208 (2007).
- [11] Silva, V. P. R., Azevedo, P. V. and Silva B. B., "Surface energy fluxes and evapotranspiration of a mango orchard grown in a semiarid environment," *Agronomy Journal*, 99(6), 1391-1396 (2007).



- [12] Zhang, B., Kang, S., Li, F. and Zhang, L., "Comparison of three evapotranspiration models to Bowen ratio-energy balance method for a vineyard in an arid desert region of northwest China," *Agricultural and Forest Meteorology*, 148(10), 1629-1640 (2008).
- [13] Di Pace, F. T.; Silva, B. B. and Silva, V. P. R.; Silva, S. T. A., "Mapeamento do saldo de radiação com imagens Landsat 5 e modelo de elevação digital," *Revista Brasileira de Engenharia Agrícola e Ambiental*, 12(4), 385-392 (2008).
- [14] Gomes, H. B., Silva, B. B., Cavalcanti, E. P. and Rocha, H. R., "Balanço de radiação em diferentes biomas no Estado de São Paulo mediante imagens Landsat 5," *Geociências*, 28, 153-164 (2009).
- [15] Bisht G., Venturini V., Islam S. and Jiang L., "Estimation of the net radiation using MODIS (Moderate Resolution Imaging Spectroradiometer) data for clear sky days," *Remote Sensing of Environment*, 97, 52 – 67 (2005).
- [16] Islam, S., Eltahir, E. and Jiang, L., [Final report on satellite based evapotranspiration estimation for South Florida Water Management District], Florida, 74p (2003).
- [17] Bastiaanssen, W. G. M., Menenti, M., Feddes, R. A. and Holtslag, A. A. M., "A remote sensing surface energy balance algorithm for land (SEBAL) I. Formulation," *Journal of Hydrology*, 212–213, 198–212 (1998).
- [18] Gilman, K., "Estimating the soil heat flux in an upland drainage basin," *Hydrological Sciences-Bulletin-des Sciences Hydrologiques*, 25(4), 435-451 (1980).
- [19] Hill, J. and Mégier, J., [Imaging Spectrometry - a Tool for Environmental Observations], Kluwer Academic Publishers, Dordrecht, 87p (1994).
- [20] Ben-Dor, E. and Banin, A., "Near infrared analysis (NIRA) as a simultaneously method to evaluate spectral featureless constituents in soils," *Soil Science*, 159, 259–269 (1995).